Title	Shear stress inhibits IL-17A-mediated induction of osteoclastogenesis via osteocyte pathways
Author(s)	LIAO, C; Cheng, T; WANG, S; Zhang, C; Jin, L; Yang, Y
Citation	Bone, 2017, v. 101, p. 10-20
Issued Date	2017
URL	http://hdl.handle.net/10722/244789
Rights	This work is licensed under a Creative Commons Attribution-NonCommercial-NoDerivatives 4.0 International License.

Bone 101 (2017) 10–20

Contents lists available at ScienceDirect

Bone

journal homepage: www.elsevier.com/locate/bone

Full Length Article

Shear stress inhibits IL-17A-mediated induction of osteoclastogenesis via osteocyte pathways

Chongshan Liao [a], Tianfan Cheng [b], Shuai Wang [c], Chengfei Zhang [c], Lijian Jin [b], Yanqi Yang [a,*]

[a] Orthodontics, Faculty of Dentistry, The University of Hong Kong, Sai Ying Pun, Hong Kong, China
[b] Periodontology, Faculty of Dentistry, The University of Hong Kong, Sai Ying Pun, Hong Kong, China
[c] Endodontology, Faculty of Dentistry, The University of Hong Kong, Sai Ying Pun, Hong Kong, China

ARTICLE INFO

Article history:
Received 26 November 2016
Revised 13 April 2017
Accepted 13 April 2017
Available online 14 April 2017

Keywords:
Interleukin-17
Osteocytes
Fluid flow
Osteoclastic differentiation
Bone remodeling

ABSTRACT

Interleukin (IL)-17 is crucial to osteoclast differentiation and activation. Osteocytes support osteoclast formation and are thought to orchestrate bone remodeling in response to fluid flow. The contribution of IL-17 to osteocyte-related bone resorption remains unclear. Here, we used the osteocyte-like MLO-Y4 cell line to examine the role of IL-17 and fluid flow in osteoclastogenesis. It was the first time to demonstrate that IL-17A promoted MLO-Y4 cell proliferation, enhanced expression of receptor activator of nuclear factor κ-B ligand (RANKL) and tumor necrosis factor-α (TNF-α), and induced osteoclastogenesis when MLO-Y4 cells were co-cultured with bone marrow-derived macrophage (BMM) cells. Additionally, shear stress upregulated osteoprotegerin expression in osteocytes, downregulated the effect of IL-17A on RANKL and TNF-α expression, and attenuated IL-17A-activated osteoclastic differentiation in the co-culture system of MLO-Y4 and BMM cells. Furthermore, we explored the signaling pathways that potentially mediate these effects in osteocytes, and found that the extracellular signal-regulated kinase (ERK)1/2 and signal transducer and activator of transcription (STAT3) pathways were suppressed by IL-17A but induced by fluid flow. EphA2 signaling enhances osteoclastogenesis in osteocytes, and the intercellular reversed EphA2-ephrinA2 signaling from osteocytes to BMM play an important role in IL-17A-dependent osteoclastic differentiation. EphB4 signaling inhibits osteoclastogenesis in osteocytes, and the intercellular reversed EphB4-ephrinB2 signaling from osteocytes to BMM could inhibit IL-17A-dependent osteoclastic differentiation. The current findings suggest that IL-17A as a promoter of bone resorption and fluid shear stress critically regulate bone remodeling via osteocyte-specific signaling pathways. IL-17 modulation-based approaches may be developed as a novel therapeutic strategy for enhancing bone remodeling efficiency and stability.

1. Introduction

Bone remodeling requires coupling between osteoclastic and osteoblastic activities and involves a dynamic balance between bone resorption and bone formation [1]. Osteocytes are believed to be responsible for detecting and responding to mechanical loading and initiating bone adaptation, and have been shown to support osteoclast formation and activation when co-cultured with osteoclast precursors [2,3]. When subjected to fluid flow, osteocytes stimulate differentiation of osteoblasts via soluble factors [4].

Mechanical compressive force has been found to induce osteoblast-like cells to overexpress IL-17 [5]. IL-17 is a cytokine family that comprises six members, IL-17A to IL-17F, which are secreted primarily by T helper 17 cells and are known to orchestrate osteoclast differentiation and activation [6,7]. Like other pro-inflammatory cytokines, IL-17 induces osteoclastogenesis via activation of the receptor activator of nuclear factor κ-B ligand (RANKL)–receptor activator of nuclear factor κ-B (RANK)–osteoprotegerin (OPG) system [8]. IL-17 recruits immune cells that express various cytokines and large amounts of RANKL [8], and also affects osteoclastic resorption indirectly by inducing osteoblasts to express IL-1, TNF-α and RANKL [6,7,9]. Blocking IL-17A with neutralizing antibodies impairs osteoclast formation in bone marrow cell/osteoblast co-culture [10].

Recently, bidirectional ephrin-Eph signaling was reported to control bone homeostasis [11]. EphrinA2-EphA2 signaling activation in osteoblasts was shown to inhibit osteoblast-specific genes (alkaline phosphatase, runt-related transcription factor 2, and Osterix), leading to bone resorption [12]. EphrinB2-EphB4 signaling is markedly activated at later stages of osteoclast differentiation, which inhibits osteoclast formation [11]. Additionally, mitogen-activated protein kinase kinase

Abbreviations: IL-17, interleukin-17; OPG, osteoprotegerin; RANKL, receptor activator of nuclear factor κ-B ligand; TNF-α, tumor necrosis factor-α; BMM, bone marrow-derived macrophage; ERK, extracellular signal-regulated kinase; STAT3, signal transducer and activator of transcription..

* Corresponding author.
E-mail address: yangyanq@hku.hk (Y. Yang).

http://dx.doi.org/10.1016/j.bone.2017.04.003

(MEK)-extracellular signal-regulated kinase (ERK)1/2 kinases have been suggested as downstream targets of the reactive oxygen species formed upon IL-17 stimulation [13]. Furthermore, the signal transducer and activator of transcription (STAT3) signaling pathway is essential for T helper 17 cell differentiation [14,15], and is required for IL-23-mediated IL-17 production in a spontaneous arthritis animal model [16]. However, pathways involved in osteocyte-specific regulation of bone resorption remain unclear. We hypothesize that ephrin-Eph, ERK1/2, and STAT3 signaling are involved in mediating the effects of mechanical stimulation in IL-17A-induced osteoclastogenesis.

To date, the role of IL-17 in bone remodeling has not been well explored. Here, we use fluid shear stress on osteocytes to simulate bone remodeling, and investigate the mechanisms of IL-17 regulation of bone resorption via osteocyte-specific signaling pathways. Our findings could help to elucidate the specific mechanisms that mediate load bearing-related bone resorption, and facilitate understanding of orthodontic tooth movement.

2. Materials and methods

2.1. Cell culture

MLO-Y4, kindly provided by Dr. Lynda Bonewald (University of Missouri-Kansas City, Kansas City, MO, USA), is an immortalized cell line with properties very similar to those of primary osteocytes in terms of morphology and expression of several important molecular osteocyte markers [17]. Cells were cultured on collagen-coated plates in α-minimum essential medium (α-MEM) (GIBCO, Grand Island, NY, USA) containing 5% fetal bovine serum (FBS) (BioWhittaker, Walkersville, MD, USA), 5% bovine calf serum (HyClone, Logan, UT, USA) and 1% penicillin and streptomycin under 5% CO_2 at 37 °C [18].

2.2. Shear stress loading

Dynamic fluid flow is a mechanical stimulus that osteocytes experience in vivo with habitual loading [19]. MLO-Y4 cells were seeded on type I rat tail collagen (BD Biosciences, Bedford, MA, USA)-coated glass slides (75 mm × 38 mm × 1 mm) at 200,000 cells/slide and cultured for 48 h to ensure 80%–90% confluence at the time of the flow experiment. Peristaltic fluid flow (PFF) was generated by a Streamer® Shear Stress Device (Flexcell, Hillsborough, NC, USA). Two-hour exposure to peristaltic fluid flow (0.7 ± 0.3 Pa, 5 Hz) was selected as the mechanical stimulus to give maximal impact on the RANKL/OPG ratio [20]. A two-speed pattern, 4 and 16 dyn/cm^2, was used to represent low and high PFF levels, respectively [21]. Six slides were placed in the flow chamber, which was placed in a CO_2 incubator for the duration of the force-loading experiment. The control samples were not exposed to flow.

2.3. Exogenous IL-17A induction and IL-17RA blocking

For exogenous treatment with mouse IL-17A (R&D Systems, Minneapolis, MN, USA), MLO-Y4 osteocytes were seeded at 10,000 cells/cm^2 in six-well plates and stimulated by IL-17A (0.5, 5, or 50 ng/mL) in α-MEM containing 2.5% FBS and 2.5% BS for up to 72 h. For the blocking assay, serum-starved MLO-Y4 cells were treated in the presence of 0.8 μg/mL IL-17A receptor neutralizing antibody (R&D Systems) for 1 h, followed by the stimulation of exogenous 50 ng/mL IL-17A. The control group was cultured in normal medium under the same conditions.

2.4. EphA2 gene silencing and EphB4 Fc chimera protein induction

MLO-Y4 cells were seeded to be 80% confluent at transfection. Lipofectamine® RNAiMAX Reagent and Silencer® pre-designed siRNA for mouse siEpha2 (#AM16708) or Silencer® Negative Control No. 1 siRNA (#AM4636) were diluted respectively in Opti-MEM® Medium and then incubated together for 5 min according to manufacturer's instructions. Cells were incubated with siRNA-lipid complex for 24 h. The final siRNA concentration was 100 nM. All transfection reagents and siRNAs were obtained from Thermo Fisher Scientific (Waltham, MA, USA). Gene knockdown was validated by western blotting.

Serum-starved MLO-Y4 cells were treated 4 μg/mL of mouse-Fc or mouse EphB4-Fc (R&D Systems) for 3 h at 37 °C as indicated. EphB4 signaling was examined by western blotting.

2.5. Magnetic cell separation from co-culture system

A co-culture of MLO-Y4 cells and mouse bone marrow-derived macrophages (BMMs) was carried out to explore the role of osteocytes in osteoclastogenesis regulation. BMMs were a gift from Dr. Chen Ling (Li Ka Shing Faculty of Medicine, HKU). The primary BMM culture was conducted as previously described [22]. Cells were collected by using trypsin from co-culture for 3 days and re-suspended in buffer to be a single-cell suspension.

In mice, the CD11b antigen is expressed on monocytes/macrophages from bone marrow [23]. CD11b$^+$ cells (BMM) were separated from cell suspension using CD11b MicroBeads, an LS Column, and a MiniMACS™ Separator according to the manufacturer's instructions (Miltenyi Biotec, Teterow, Germany). Unlabeled cells (MLO-Y4) were also collect in the flow-through buffer. Collected cells were immediately re-suspended in RNAlater® Stabilization Solution (Thermo Fisher).

2.6. Cell proliferation and apoptosis analysis

Cells were seeded in 96-well plates at 5000 cells/well. Assays were conducted six times for each experiment. Cells were stimulated with IL-17 (0.5, 5 or 50 ng/mL) for up to 72 h. Cell Counting Kit-8 (CCK-8; 10 μL per 100-μL reaction system; Sigma-Aldrich, St. Louis, MO, USA) was added to each well and the cells were incubated for 1.5 h in 5% CO_2 at 37 °C. Cell proliferation was monitored by determining absorbance at 450 nm, with 650 nm used for wavelength correction, using a SpectraMax M2 microplate reader (Molecular Devices, Orleans Drive Sunnyvale, CA, USA). Measurements were recorded at 0, 24, 48 and 72 h after IL-17A treatment.

Annexin V-FITC and PI staining were conducted according to the manufacturer's instructions. MLO-Y4 cells were seeded on six-well plates (100,000 cells/well). Cells were pretreated with fresh medium with or without IL-17A on the next day. Cells were then harvested with 0.05% trypsin at 24, 48 and 72 h after initiation of treatment, and stained with annexin V-FITC and PI according to the manufacturer's instructions (Thermo Fisher Scientific). The cells were analyzed immediately after staining using a FACSVerse flow cytometer (Becton Dickinson, San Jose, CA, USA) and FlowJo 10.2 software (Ashland, Oregon, USA). Assays were conducted three times for each experiment.

2.7. Real-time quantitative PCR (qPCR)

The total RNA isolated from each sample was reverse transcribed using SuperScript™ VILO Master Mix (Thermo Fisher Scientific) in a Veriti Thermal Cycler (Applied Biosystems, Foster City, CA, USA). PCR amplification was performed using a StepOnePlus™ Real-Time PCR System (Applied Biosystems). The copy numbers for the target genes was normalized to the copy numbers for glyceraldehyde-3-phosphate dehydrogenase (GAPDH). Expression of IL-17, IL-17R, OPG/RANKL and TNF-α mRNA was evaluated. The primer sequences are shown in Table 1.

2.8. Ephrin–Eph immunofluorescence imaging

PFF-treated MLO-Y4 cells on glass slides were fixed in 4% paraformaldehyde in PBS and blocked with goat serum. Two groups of cells (A and B) were then incubated with primary antibodies (group A: rabbit anti-ephrinA2 (1:200; Santa Cruz), mouse anti-EphA2

Table 1
Primers used in real-time polymerase chain reaction gene expression analysis.

Gene	Primer sequences (5′-3′)
GAPDH	
Forward	GCATCTCCCTCACAATTTCCA
Reverse	TGCAGCGAACTTTATTGATGGT
IL-17A	
Forward	ACCGCAATGAAGACCCTGAT
Reverse	ATGTGGTGGTCCAGTTTCC
IL-17AR	
Forward	TCAGGGCCAGTGTGAAAACA
Reverse	CATGTCGGGTTATCAGGGAAA
RANKL	
Forward	TGGGCCAAGATCTCTAACATGA
Reverse	CATGATGCCGAAAGCAAATG
OPG	
Forward	CGAGAAAGACCTGCAAATCGA
Reverse	GCATACATCAGGCCCTTCAAG
TNF-α	
Forward	ATGAGCACAGAAAGCATGATC
Reverse	TACAGGCTTGTCACTCGAATT
EphrinA2	
Forward	GCCACAGGGATGAGGTGAA
Reverse	GGACCAAATAACAGGACACAGA
EphrinB2	
Forward	TCGGTTGGCTACGTTTTGGT
Reverse	ACGCACAGGACACTTCTCAATG

(1:200; Santa Cruz); group B: rabbit anti-ephrinB2 (1:200; Abcam) and rat anti-EphB4 (1:100; Abcam)) and fixed at 4 °C in a humidified box overnight. Group A cells were then incubated with Alexa Fluor 488 goat anti-rabbit IgG (1:500; Abcam) and Alexa Fluor 647 goat anti-Mouse IgG (1:500; Abcam), and group B cells were incubated with Alexa Fluor 488 goat anti-rabbit IgG (1:500; Abcam) and Alexa Fluor 647 goat anti-rat IgG (1:500; Abcam) at 37 °C in a humidified box for 2 h. All cells were then stained in DAPI for 10 min. Images were acquired using a Carl Zeiss LSM 780 fluorescence microscope (Jena, Germany) and five visual fields on each slide were randomly selected. The images were processed using Zen 2 core Software (Carl Zeiss).

2.9. Western blotting

Cell lysates was prepared using RIPA cell-lysis buffer (Thermo Fisher Scientific). Total protein concentration was determined using the BCA reagent system (Thermo Fisher Scientific). Protein extracts (20 μg of total cell proteins) were subjected to 7.5% to 15% SDS-PAGE and electrotransferred onto polyvinylidene difluoride membrane. Nonspecific binding was blocked using Tris-buffered saline with 0.5% Tween 20 containing 5% skimmed milk powder. Specific antigens were immunodetected using appropriate primary and secondary antibodies and visualized using enhanced chemiluminescence detection reagents (ECL Plus; GE Healthcare, London, UK). The membranes were stripped using Restore Western Blot Stripping Buffer (Thermo Fisher Scientific) and reprobed for β-actin or GAPDH to confirm that equivalent amounts of proteins had been loaded and transferred. The primary antibodies were: rabbit anti-RANKL (1:500, Santa Cruz), rabbit anti-ERK1/2 (1:1000, Cell Signaling Technology), rabbit anti-pERK1/2 (1:1000, Cell Signaling Technology), rabbit anti-STAT3 (1:1000, Cell Signaling Technology), rabbit anti-pSTAT3 (1:1000, Cell Signaling Technology), rabbit anti-STAT3 (1:1000, Cell Signaling Technology), rabbit anti-ephrinA2 (1:1000; Santa Cruz), mouse anti-EphA2 (1:1000; Santa Cruz), rabbit anti-ephrinB2 (1:1000; Abcam), rat anti-EphB4 (1:1500; Abcam), rabbit anti-GAPDH (1:1000, Cell Signaling Technology), and rabbit anti-β-actin (1:1000, Cell Signaling Technology). Secondary antibodies were all obtained from Cell Signaling Technology (1:3000).

2.10. Enzyme-linked immunosorbent assay (ELISA)

PFF-treated cells were cultured in 4-well dishes in fresh medium for another 24 h with or without IL-17A. The media were collected and centrifuged to removal cell debris. IL-17A, OPG, sRANKL and TNF-α levels in the culture supernatants were measured by ELISA (all kits from R&D Systems) according to the manufacturer's instructions. The optical density of each well was determined using a SpectraMax M2 microplate reader at to determine absorbance at 450 nm, with 540 nm used for wavelength correction.

2.11. TRAP staining of co-culture system for Osteoclastogenesis

MLO-Y4 cells were seeded at 500 cells/cm^2 in collagen-coated 12-well plates (day 0). BMMs were added at 2500 cells/cm^2 at day 2 and then co-cultured in DMEM containing 5% FBS with or without 50 ng/mL IL-17 for 7 days. Media were changed every 2 days. On day 7 after BMM plating, cells were fixed and stained for tartrate-resistant acid phosphatase (TRAP) using a leukocyte acid phosphatase kit (Sigma-Aldrich). Cells were imaged using a light microscope with a 20× objective, and counted by 2 blinded investigators. TRAP$^+$ cells were counted and classified as mononuclear, multinuclear (2–10 nuclei), or giant cells (≥10 nuclei), as described previously [24,25].

The effect of soluble factors released by osteocytes on osteoclastogenesis was studied using conditioned media from MLO-Y4 cells. After flow exposure, cell on glass slides were transferred to 4-well sterile dishes (Thermo, Rochester, NY, USA) with 4 mL of fresh media added. At 24 h after flow exposure, conditioned media were collected and added immediately to the BMM/MLO-Y4 co-culture to replace 50% of the original culture media. Media from osteocytes not treated with PFF were also collected. This process was repeated every day until day 7.

We also used conditioned media for indirect co-culture. BMMs were seeded at 2500 cells/cm^2 in collagen-coated 12-well plates and cultured in four kinds of conditioned media: medium from osteocytes, medium from osteocytes treated with IL-17A, medium from osteocytes treated with PFF, and medium from osteocytes pretreated with PFF in the presence of IL-17A. Media were changed daily until day 7.

2.12. Statistical analysis

One way analysis of variance (ANOVA) was used to compare data from more than two groups. Two significance levels, $p \le 0.05$ (*) and $p \le 0.01$ (**), were used throughout the statistical analysis. The data are reported as means ± SD. Each experiment was repeated at least three times independently.

3. Results

3.1. IL-17A induced MLO-Y4 cell proliferation but did not affect apoptosis

IL-17A enhanced the proliferation of MLO-Y4 after 48 h incubation in a concentration-dependent manner, with the greatest effect observed for 50 ng/mL IL-17A (Supplementary Fig. 1A). However, the IL-17A induction had no significant effect on MLO-Y4 apoptosis (Supplementary Fig. 1B).

3.2. Osteoclastogenic factor expression was downregulated by PFF but enhanced by IL-17A; while the effect of IL-17A was attenuated by PFF stimulation in MLO-Y4 cells

To investigate the potential effect of PFF on bone remodeling in MLO-Y4 cells, the expression of RANKL and OPG was investigated. OPG mRNA expression and secretion was significantly enhanced after force application (Fig. 1A and B), whereas secreted RANKL (sRANKL) levels decreased (Fig. 1B). The decrease in RANKL/OPG mRNA and the

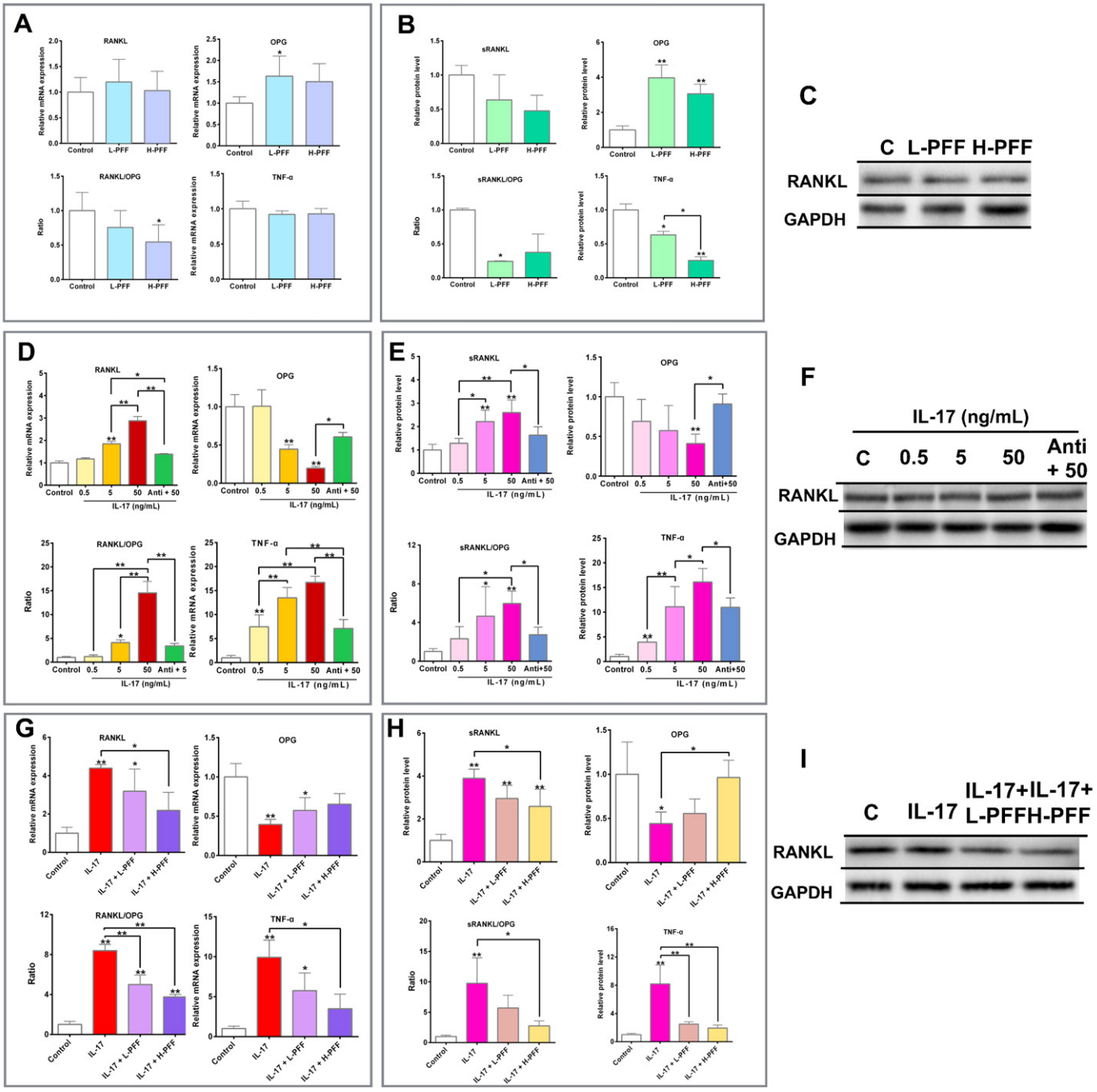

Fig. 1. Peristaltic fluid flow (PFF) and IL-17A regulated osteoclastogenesis by regulating RANKL, OPG, and TNF-α in MLO-Y4 osteocytes. q-PCR (A) and ELISA (B) analysis of RANKL, OPG and TNF-α mRNA expression and RANKL/OPG ratio in cells treated with low-PFF (L-PFF) and high-PFF (H-PFF) for 2 h. (C) Western blot analysis of membrane-bound RANKL expression after shear stress. q-PCR (D) and ELISA (E) analysis of RANKL, OPG and TNF-α mRNA expression, and RANKL/OPG ratio in cells treated with 0.5, 5, or 50 ng/mL IL-17A, or 0.8 μg/mL IL-17RA antibody + 50 ng/mL IL-17A. (F) Western blotting analysis of membrane-bound RANKL expression treated with IL-17A with or without anti-IL-17RA. q-PCR (G) and ELISA (H) analysis of RANKL, OPG and TNF-α mRNA expression, and RANKL/OPG ratio in cells treated with 50 ng/mL IL-17A with or without L-PFF or H-PFF pretreatment. (I) Western blotting analysis of membrane-bound RANKL expression treated with 50 ng/mL IL-17A with or without PFF pretreatment (bars represent means ± SD from 3 independent studies, $^{*}p < 0.05$, $^{**}p < 0.01$).

sRANKL/OPG ratio suggest downregulation of osteoclastogenesis. TNF-α, which promotes osteoclast differentiation directly or indirectly [26], significantly downregulated by PFF; this further confirms that shear stress can suppress osteoclastogenic differentiation. It was particularly notable that high PFF had stronger effects on secretion of TNF-α than low PFF (Fig. 1B).

The effect of IL-17A on bone remodeling factors in MLO-Y4 was also investigated. Addition of IL-17A to MLO-Y4 cells increased in RANKL mRNA expression and sRANKL secretion, thereby leading to a marked RANKL/OPG ratio increase. Enhanced TNF-α expression also indicated the osteoclastogenic effect of IL-17A. Antibodies against the IL-17A receptor were used to block IL-17A. The effects of 50 ng/mL IL-17A on RANKL/OPG ratio and TNF-α were attenuated by anti-IL-17RA antibody (0.8 μg/mL) (Fig. 1D, E).

We next investigated the effect of IL-17A on MLO-Y4 cells after mechanical stimulation. PFF pretreatment significantly attenuated

the IL-17A-induced increase in RANKL/OPG mRNA ratio and sRANKL/OPG ratio, and also attenuated the IL-17A-induced increase in TNF-α mRNA and protein levels (Fig. 1G, H). No evident change was observed in membrane-bound RANKL expression caused by either PFF or IL-17 or these two inductions together (Fig. 1C, F, I).

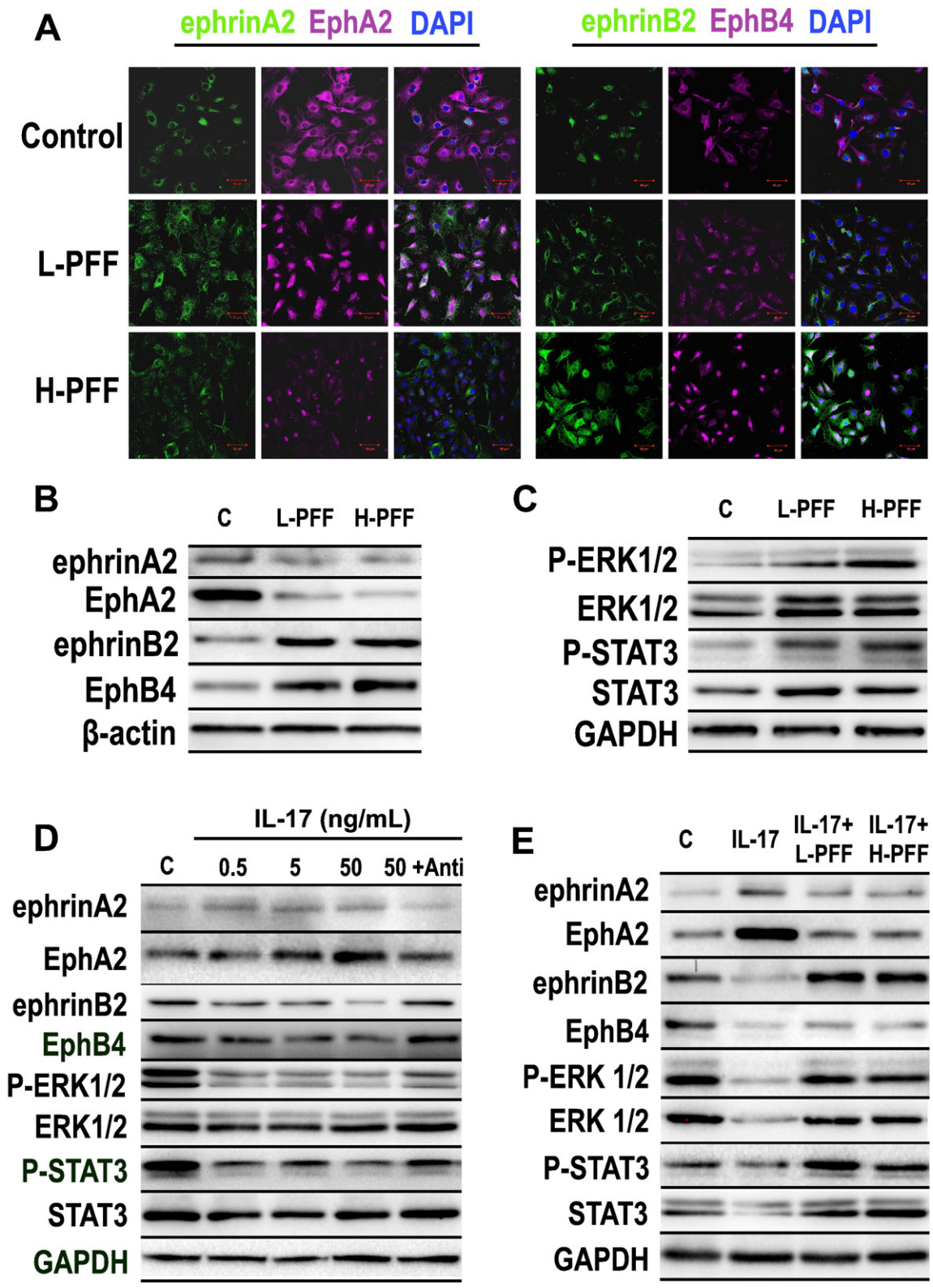

Fig. 2. Ephrin-Eph, STAT3 and ERK1/2 signaling were regulated in MLO-Y4 cells subjected to shear stress and IL-17A treatment. (A) Immunofluorescence staining of ephrinA2 (green)-EphA2 (red) and ephrinB2 (green)-EphB4 (red) in osteocytes treated with L-PFF or H-PFF for 2 h. Nuclei were stained with DAPI (blue). Bar = 50 μm. (B) Western blotting analysis of ephrinA2–EphA2, ephrinB2–EphB4, P-ERK1/2, ERK1/2, P-STAT3 and STAT3 treated with PFF for 2 h (B and C), or treated with 0.5, 5 or 50 ng/mL IL-17A, or 50 ng/mL IL-17A + 0.8 μg/mL IL-17RA antibody (D), or treated with 50 ng/mL IL-17A with or without 2 h PFF pretreatment (E).

3.3. Ephrin-Eph, ERK1/2 and STAT3 signaling was regulated by PFF or IL-17A, while PFF antagonized IL-17A regulation in MLO-Y4 cells

To investigate the retroactive mechanism of PFF simulation on MLO-Y4 cells, ephrin-Eph, ERK1/2 and STAT3 signaling were analyzed. Ephrin-Eph localization was confirmed by immunofluorescence imaging, which indicated that ephrinA2-EphA2 and ephrinB2-EphB4 were located on the membrane of MLO-Y4 cells, and could be expressed in the nuclei after force loading (Fig. 2A). After PFF treatment, ephrinA2 and EphA2 expression was decreased, whereas ephrinB2 and EphB4 expression was increased (Fig. 2B). Additionally, PFF increased P-ERK1/2 and P-STAT3 but not ERK1/2 and STAT3, indicating that PFF activated the two pathways by facilitating ERK1/2 and STAT3 phosphorylation (Fig. 2C).

Furthermore, ephrinA2-EphA2 signaling was activated by increasing exogenous IL-17A (0.5, 5 or 50 ng/mL), while IL-17A suppressed ephrinB2-EphB4 signaling (Fig. 2D). Additionally, P-ERK1/2 and P-STAT3 levels were decreased with increasing IL-17A. In the blocking assay, anti-IL-17RA antibody counteracted the effects of IL-17A on ephrinA2-EphA2, ephrinB2-EphB4 and P-ERK1/2 and P-STAT3 levels.

The IL-17A-dependent activation of ephrinA2-EphA2 signaling was attenuated by PFF pretreatment, whereas the IL-17A-mediated

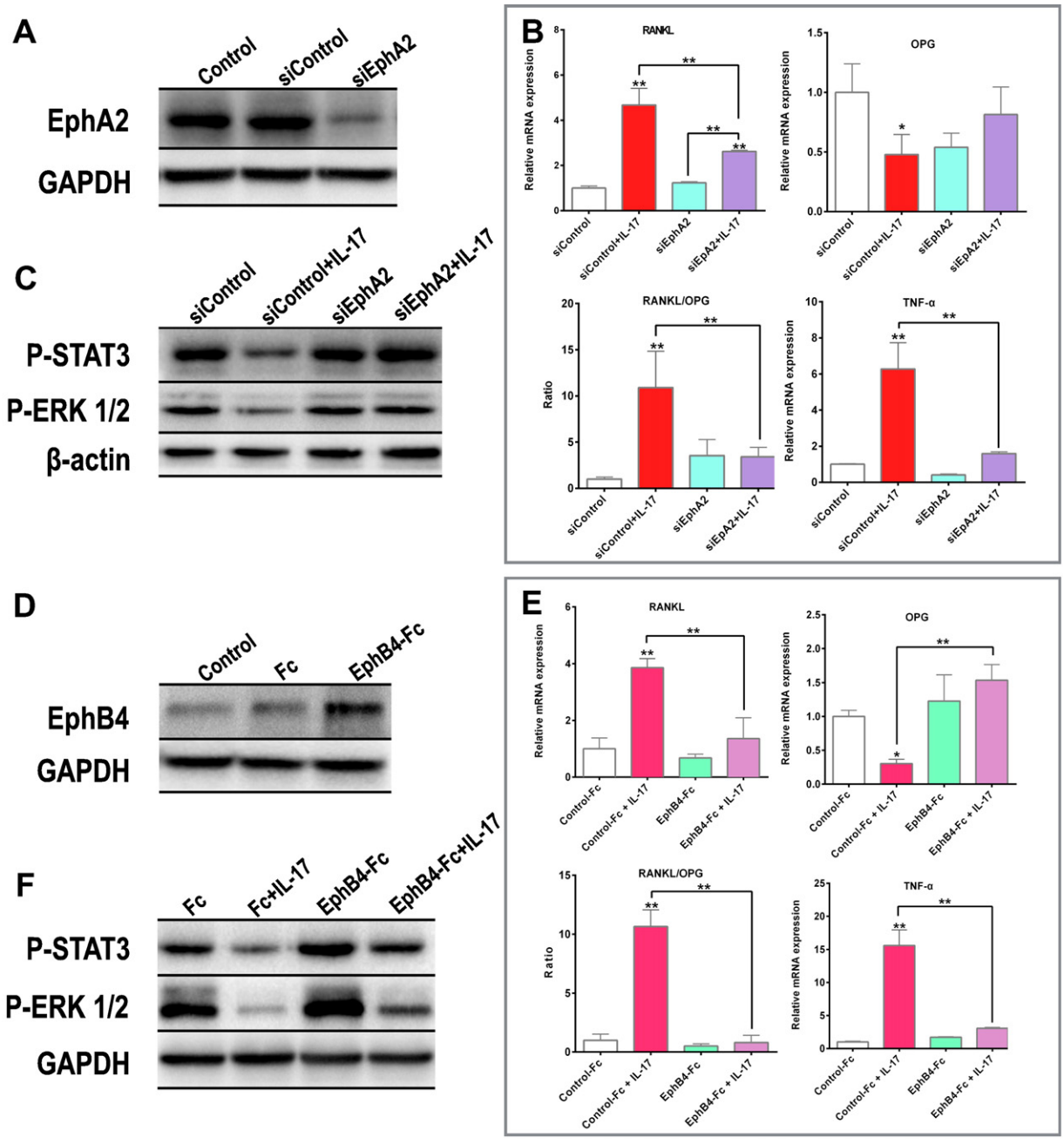

Fig. 3. Inhibited EphA2 signaling and enhanced EphB4 signaling attenuated IL-17-dependent osteoclastogenesis. (A) Western blotting analysis of EphA2 after siEphA2 transfection for 24 h. (B) qPCR analysis of RANKL, OPG and TNF-α mRNA expression and RANKL/OPG ratio in cells treated with siControl or siEphA2 with or without IL-17A. (C) Western blotting analysis of P-ERK1/2 and P-STAT3 treated with siControl or siEphA2 with or without IL-17A. (D) Western blotting analysis of EphB4 after EphB4-Fc treatment for 3 h. (E) qPCR analysis of RANKL, OPG and TNF-α mRNA expression and RANKL/OPG ratio in cells treated with Control-Fc or EphB4-Fc with or without IL-17A. (F) Western blotting analysis of P-ERK1/2 and P-STAT3 treated with Control-Fc or EphB4-Fc with or without IL-17A.

reduction in ephrinB2-EphB4 signaling was enhanced by PFF pretreatment (Fig. 2E). Similarly, the IL-17A-dependent inhibition of P-ERK1/2 and P-STAT3 was reversed by 2-hour PFF stimulation (Fig. 2E).

3.4. Intracellular EphA2 and EphB4 signaling regulated IL-17-dependent osteoclastogenesis in osteocytes

The effect of EphA2 knockdown in MLO-Y4 cells by siRNA was confirmed by western blotting analysis (Fig. 3A). The knockdown of EphA2 significantly decreased IL-17-stimulated RANKL and TNF-α, thereby leading to the decreasing of RANKL/OPG ratio (Fig. 3B), indicating that EphA2 signaling plays an important role in IL-17 downstream pathway. We further investigated whether EphA2 signaling mediated IL-17 pathway via STAT3 or ERK1/2 (Fig. 3C). The reduced expression of P-STAT3 and P-ERK1/2 caused by IL-17 was reversed by siEphA2, however, the knockdown of EphA2 had no direct effect on STAT3 and ERK1/2 signaling (Fig. 3C).

EphB4-Fc was used to enhance EphB4 signaling in osteocytes (Fig. 3D). The enhanced EphB4 signaling significantly down-regulated IL-17-sitmulated RANKL and TNF-α and up-regulated IL-17-inhibited OPG expression, thereby, leading to the decrease of RANKL/OPG ratio (Fig. 3E). The above results indicated that EphB4 signaling was involved in osteoclastogenic pathway of IL-17. We further investigated the role of EphB4-Fc on STAT3 and ERK1/2 signaling, which showed that EphB4-Fc could enhance P-STAT3 and P-ERK1/2 notably and further attenuated the effect of IL-17 (Fig. 3F). Hence, EphB4 signaling could inhibit osteoclastogenic pathway of IL-17 via STAT3 or ERK1/2.

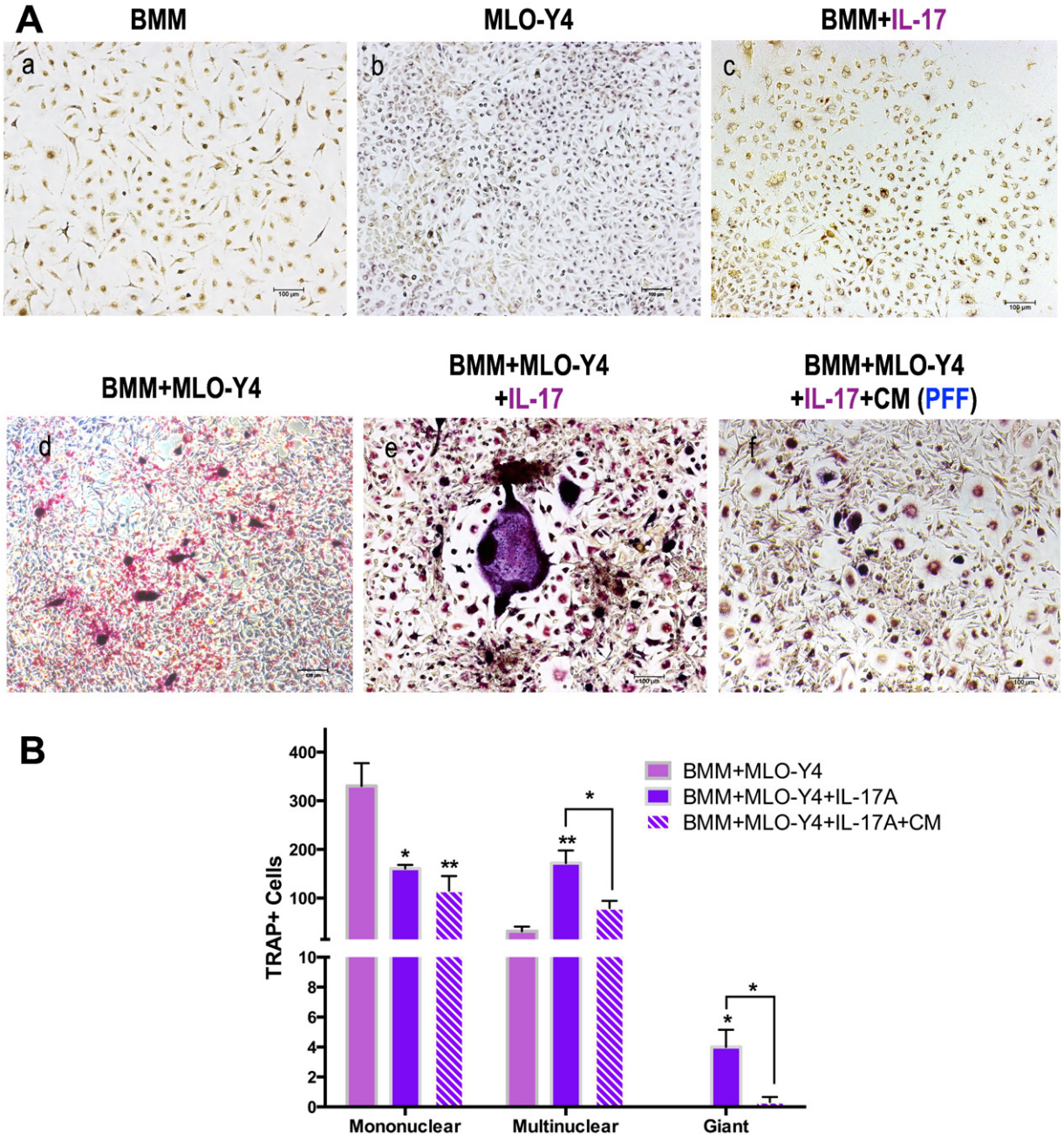

Fig. 4. Osteoclastic differentiation in direct co-culture of MLO-Y4 cells and BMMs for 7 days. No $TRAP^+$ cells were observed in BMM-only (A-a) or MLO-Y4-only (A-b) or BMM-only treated with IL-17 (A-c). BMM and MLO-Y4 cell co-culture in normal α-MEM medium (A-d), or treated with 50 ng/mL IL-17A(A-e), or treated with 50 ng/mL IL-17A in conditioned medium from MLO-Y4 cells pretreated with H-PFF (A-f). Bar = 100 μm. Percentage values for mononuclear, multinuclear and giant $TRAP^+$ cells were derived from three independent experiments (B).

3.5. IL-17A promoted osteoclastogenesis in a MLO-Y4 and BMM co-culture system, which was attenuated by PFF

To verify the function of IL-17A in osteoclastogenesis, we co-cultured MLO-Y4 osteocytes with BMM osteoclast precursors. Comparing with BMM or MLO-Y4 cell culture (Fig. 4A-a and b), TRAP staining showed that the osteocytes facilitated osteoclast formation in the co-culture system in the absence of exogenous RANKL (Fig. 4A-d). IL-17A significantly promoted multinuclear and giant TRAP$^+$ cells (Fig. 4A-e) in co-culture rather than in single BMM cells (Fig. 4A-c). Additionally, conditioned medium from 2-hour flow exposure appeared to diminish the osteoclastic effect of IL-17A, with fewer multinuclear and giant TRAP$^+$ cells formed in the co-culture system (Fig. 4A-e). Percentage values for TRAP$^+$ mononuclear, multinuclear and giant cells were derived (Fig. 4B).

Indirect co-culture was performed to explore the effect of soluble factors secreted by osteocytes on osteoclastic differentiation in the absence of direct cell–cell contact with osteoclast precursors. However, no TRAP$^+$ multinuclear cells were observed when BMMs were exposed to fresh MLO-Y4 conditioned medium for 7 days (Supplementary Fig. 2B-b). Additionally, IL-17A did not induce formation of a TRAP$^+$ cell population in this indirect co-culture system (Supplementary Fig. 2B-c). Conditioned medium from PFF-pretreated MLO-Y4 cells had no apparent effects on differentiation of BMMs in either the presence or absence of IL-17A (Supplementary Fig. 2B-d and e). This indicates that the soluble factors secreted by MLO-Y4 cells were not sufficient to induce BMMs to differentiate into TRAP$^+$ cell, even with IL-17A stimulation.

3.6. Intercellular EphA2-ephrinA2 and EphB4-ephrinB2 signaling between osteocytes and BMM mediated osteoclastogenesis

The differences of expression of osteoclastogenic factors between osteocytes and BMM showed that RANKL and OPG were more

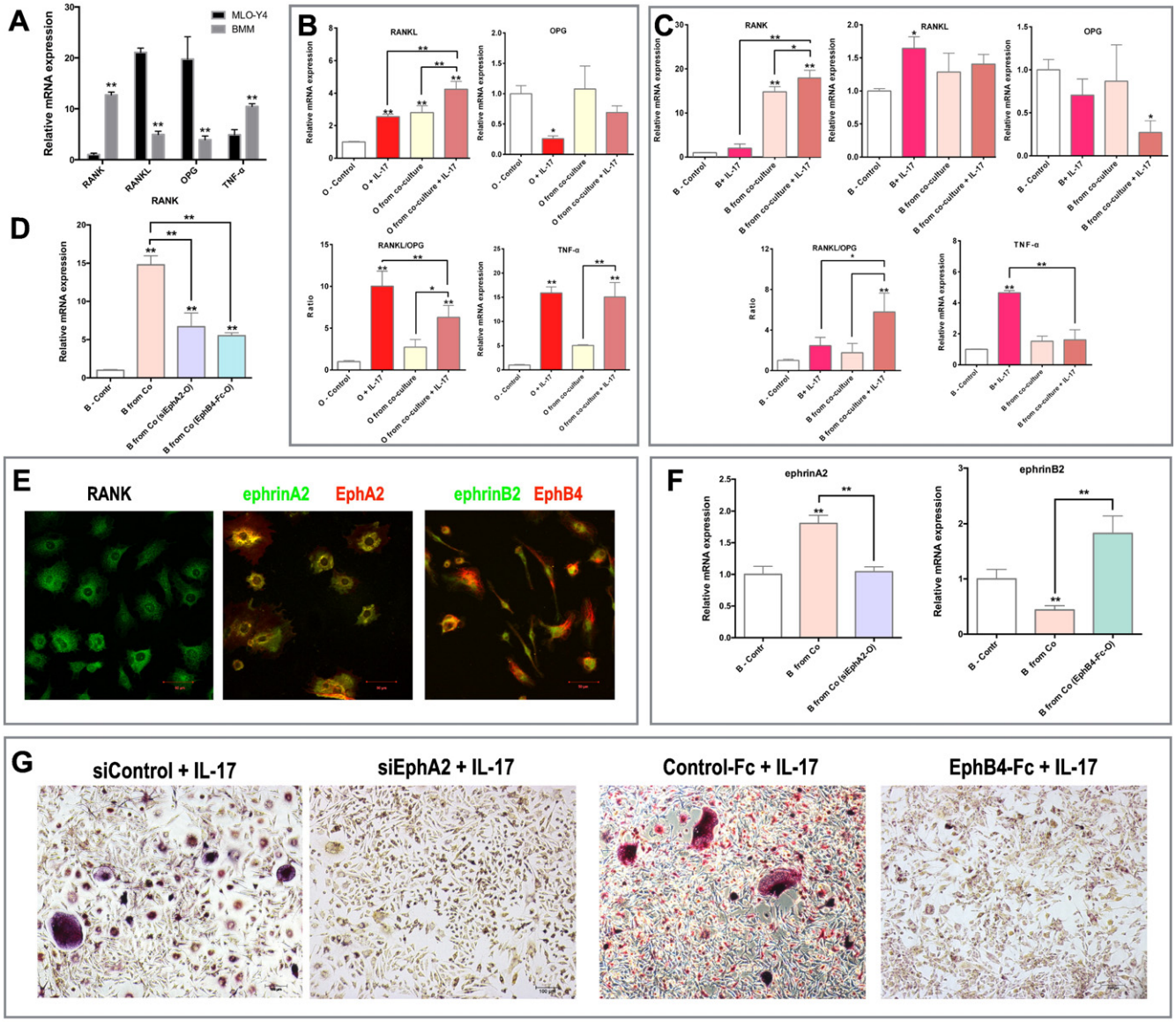

Fig. 5. Intercellular reversed Eph-Ephrin signaling mediated osteoclastogenesis. (A) qPCR analysis of RANK, RANKL, OPG and TNF-α in MLO-Y4 and BMM cells. (B) qPCR analysis of RANKL, OPG and TNF-α in MLO-Y4 after cell separation from co-culture with or without IL-17 induction. (C) qPCR analysis of RANK, RANKL, OPG and TNF-α in BMM after cell separation from co-culture with or without IL-17 induction. (D) qPCR analysis of RANK in separated BMM after co-culture with siEphA2 or EphB4 pretreated osteocytes. (E) Immunofluorescence staining of RANK, ephrinA2 (green)-EphA2 (red) and ephrinB2 (green)-EphB4 (red) in BMM. Bar = 50 μm. (F) qPCR analysis of ephrinA2 and ephrinB2 in separated BMM after co-culture with siEphA2 or EphB4 pretreated osteocytes. (G) TRAP staining of co-culture of BMM with siEphA2 or EphB4 pre-treated osteocytes for 7 days with IL-17 induction.

expressed in osteocytes compared with BMM, while RANK was highly expressed in BMM (Fig. 5A). After 72 h-co-culture, $CD11b^+$ BMM was selected from co-culture cells by magnetic cell separation and changes in expression of these osteoclastogenic factors were analyzed after magnetic cell separation (Fig. 5B and C). Attractively, RANKL in osteocytes significantly up-regulated after co-culture and even higher with IL-17 induction (Fig. 5B); while similar pattern could be found in RANK in BMM from co-culture, even more apparently (Fig. 5C).

Based on the importance of RANKL–RANK–OPG system in bone remodeling, we further focused on RANK in BMM and verified the intercellular effects of EphA2 and EphB4 signaling from osteocyte. It was shown that the inhibited EphA2 and enhanced EphB4 signaling could significantly decrease RANK expression after co-culture (Fig. 5D). Localization of RANK, EphrinA2, EphA2, EphrinB2 and EphB4 on BMM was confirmed by immunofluorescence imaging (Fig. 5E). EphrinA2 mRNA expression significantly increased after co-culture and could be counteracted by inhibiting EphA2 signaling from osteocytes, and similarly, enhanced EphB4 signaling in osteocytes could reverse the reduction of ephrinB2 expression caused by co-culture (Fig. 5F). Lastly, we verified the role of reversed Eph-ephrin signaling in IL-17 induced co-culture. EphA2-knockdown osteocytes and EphB4-Fc-osteocytes could not assist the osteoclastic differentiation of BMM even with IL-17 stimulation (Fig. 5G). Hence, intercellular reversed EphA2-ephrinA2 and EphB4-eprinB2 signaling could play an important role in osteoclastic differentiation.

4. Discussion

In this study, we demonstrated that exogenous IL-17A accelerated osteocyte proliferation after 48 h, with no significant effects on cell apoptosis until 72 h, consistent with previous studies on IL-17-induced proliferation in various cells with different origins [13,27,28]. Furthermore, exogenous IL-17A increased $TRAP^+$ multinuclear cells in a co-culture system of MLO-Y4 osteocytes and BMM osteoclast precursors, but could not induce osteoclastic differentiation of BMMs in the absence of osteocytes (Fig. 4A), indicating that IL-17A may orchestrate bone resorption via osteocyte-specific signaling pathways.

IL-17 plays roles in bone erosion via activation of RANKL–RANK–OPG system [29]. RANKL exists in two forms: membrane-bound and secreted ones, both of which regulate osteoclastogenesis [30]. IL-17 has been shown to induce macrophage colony-stimulating factor (M-CSF) and RANKL expression in human mesenchymal stem cells, thereby supporting osteoclastogenesis, both in vitro and in vivo [13]. In our study, IL-17A-induced enhancement of RANKL mRNA and sRANKL levels and increased RANKL/OPG ratio (Fig. 2D, E), indicating osteoclastic differentiation.

Oscillatory fluid flow has an anti-osteoclastogenic effect on the RANKL/OPG signaling axis in osteocytes, and decreases the osteoclastogenesis-supporting potential of MLO-Y4 cells co-cultured with RAW264.7 pre-osteoclasts [3]. Osteocytes subjected to PFF also stimulate osteoblasts differentiation in vitro via soluble factors [4]. Consistently, we found that OPG was upregulated by PFF, which led to decreased RANKL/OPG ratio, indicating inhibition of osteoclastogenesis. Importantly, we demonstrated that the osteoclastogenic activity of IL-17A was attenuated by PFF-conditioned medium (Fig. 4A-e). This may result from the increased OPG caused by PFF, as binding of OPG to RANKL not only blocks osteoclastogenesis, but also decreases survival of pre-existing osteoclasts [30].

Osteoclast formation in vivo is thought to be induced by direct cell–cell contact of pre-osteoblastic/stromal cells with monocyte/macrophage osteoclast precursors [30,31]. We found that $TRAP^+$ multinuclear cells were formed in vitro in direct co-culture of BMMs with MLO-Y4 (Fig. 4A), mainly due to membrane-bound RANKL of MLO-Y4, which constitutes the major physiological regulator of osteoclastogenesis [32,33]. Moreover, the formation of $TRAP^+$ multinuclear cells in indirect co-culture could not induced by sRANKL. sRANKL was secreted from osteocytes under physiological conditions, and could be downregulated by mechanical stimulation, or increased by exogenous IL-17A. Hence, the soluble factors released by IL-17A- and mechanically-stimulated osteocytes were not the major regulators of osteoclastogenesis, but they were able to regulate osteoclastic differentiation when accompanied by other supporting cells including bone marrow macrophages. However, it was previously demonstrated that IL-17 induced osteoclastogenesis in cultures of human CD11b-positive cells in the absence of osteoblasts or exogenous RANKL [34]. This discrepancy could result from the fact that IL-17 upregulates RANK expression in osteoclast precursors to sensitize them to RANKL [7], but the effectiveness of this process may differ in different precursor cells.

The mechanism of IL-17 stimulation of bone resorption via osteocyte-specific pathways in the presence and absence of shear stress remains unclear. Previous studies indicated that EphA2 can be upregulated by IL-17A in keratinocytes [35]. Here, we demonstrated that IL-17A activated ephrinA2-EphA2 signaling, leading to osteoclastic differentiation. Mechanical compressive force has been shown to upregulate ephrinA2 and EphA2 expression in periodontal ligament fibroblasts [36]. In our study, when osteocytes were exposed to PFF, ephrinA2 and EphA2 expression was downregulated, leading to osteoblastic differentiation, which weakened the osteoclastic effect of IL-17A. When EphA2 signaling was silenced by siRNA, IL-17-dependent RANKL in osteocytes and RANK in BMM selected from co-culture were decreased (Figs. 3D and 5B), which revealed the osteoclastogenic role of EphA2 signaling in osteocytes and from osteocytes to BMM. The down-regulation of ephrinA2 expression in BMM furtherly verified the existence of intercellular reversed EphA2-ephrinA2 signaling. This is the first time that EphA2-ephrinA2 signaling has been reported to regulate osteocytes and BMMs in osteoclastogenesis.

Mechanical strain upregulates ephrinB2 in periodontal ligament fibroblasts, contributing to osteogenesis at sites of tension in orthodontic tooth movement [37]. Consistently, we identified that IL-17A suppressed ephrinB2-EphB4 signaling, which was weakened by shear stress. Enhancing EphB4 signaling in osteocytes decreased IL-17-dependent RANKL and TNF-α expression and activated STAT3 and ERK 1/2 signaling (Fig. 3E and F), and the intercellular reverse signaling from EphB4 to ephrinB2 led to the reduction of RANK in BMM, which may explain the inhibition of osteoclastic differentiation in the co-culture system (Fig. 5F).

In our study, IL-17A decreases the contents of P-ERK1/2, which has been suggested as the downstream target for IL-17A. An in vivo model of tooth movement previously indicated enhanced P-ERK1/2 contents under tension [38]. In vitro, fluid shear stress has been shown to activate ERK1/2 in human umbilical vein endothelial cells [39]. Similarly, we found that fluid flow stimulated P-ERK1/2 production. Hence, the mechanism for promotion or inhibition of bone resorption could involve IL-17A-mediated inhibition or flow-mediated activation of ERK1/2 in osteocytes.

Loss-of-function mutation of STAT3 in osteoblasts and osteocytes has been shown to diminish load-driven bone formation [40]. We found that the phosphorylation of STAT3 (P-STAT3) was inhibited by IL-17A and activated by PFF in osteocytes, indicating STAT3 involvement in the signaling pathway downstream of IL-17A and shear stress stimulation. However, it has been demonstrated that STAT3 activation in osteoblasts is required for RANKL induction and osteoclastogenesis [41]. It is possible that there is some crosstalk between osteoblasts and osteocytes. Hence, ephrin-Eph, ERK1/2 and STAT3 signaling are involved in the effect of IL-17A on osteoclastogenesis under mechanical stimulation.

Croes et al. recently has reported that IL-17A and IL-17F similarly exhibited strong osteogenic effects when exposed directly to human mesenchymal stem cell [42]. In future, the role of IL-17A in osteoblastic differentiation and forward ephrin-Eph signaling need to be investigated and in vivo orthodontic models should be used to verify our findings regarding IL-17A-mediated bone remodeling.

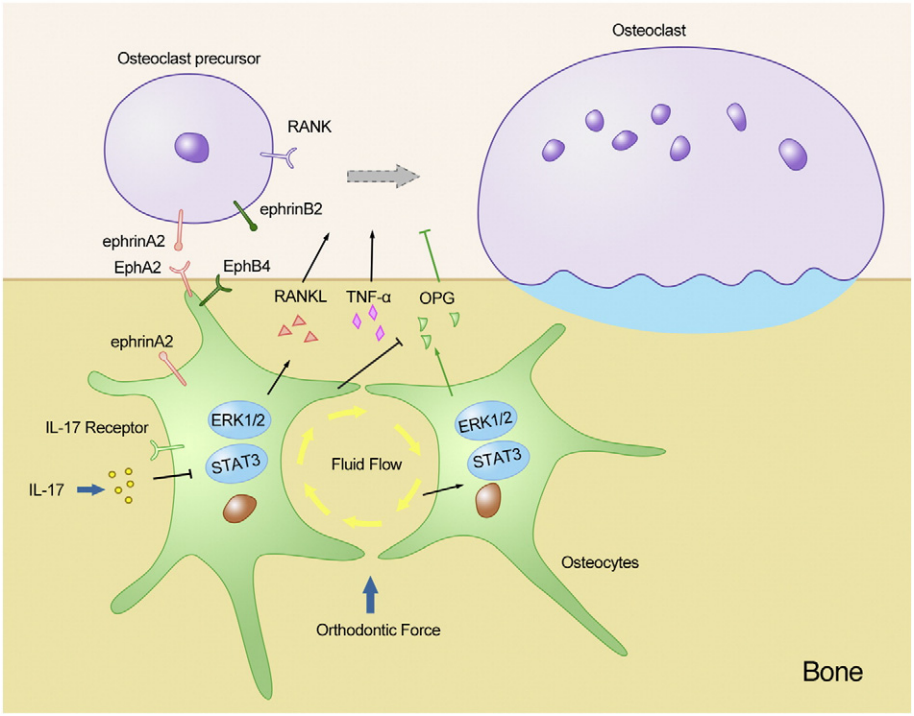

Fig. 6. Scheme of the findings of this study. IL-17A induced osteoclastic differentiation by activating the RANKL/OPG system and TNF-α in osteocytes in the presence of direct cell–cell contact with osteoclast precursors. During osteoclastogenesis, suppression of the ERK1/2 and STAT3 pathways in osteocytes and activation of reversed Eph-ephrin signaling between osteocytes and osteoclast precursors played roles downstream of IL-17A. Fluid flow through canaliculi surrounding the osteocytes stimulated biochemical responses, resulting in inhibition of osteoclastogenesis mainly due to increased OPG. ERK1/2 and STAT3 pathway activity was enhanced and ephrin-Eph signaling was regulated by fluid flow, which may ultimately attenuate the osteoclastic effect of IL-17A.

In summary (Fig. 6), we have demonstrated that IL-17A, a potential inducer of osteoclastic differentiation, enhanced $TRAP^+$ multinuclear cells formation induced by cell–cell contact between osteocytes and osteoclast precursors; PFF suppressed osteoclastic differentiation and decreased $TRAP^+$ multinuclear cells formation via soluble factors secreted by osteocytes; importantly, the effect of IL-17A on osteoclastogenesis was reduced by peristaltic fluid flow; furthermore, the ephrin-Eph, ERK1/2 and STAT3 pathways may be involve in signaling from osteocytes to osteoclast precursors, which represents the beginning of the remodeling cycle. This finding represents a novel osteocyte regulation mechanism and offers unique insight into the regulation of bone remodeling during orthodontic tooth movement. Interventions of IL-17 may contribute to novel therapeutic strategies for bone remodeling with increased treatment efficiency and stability.

Supplementary data to this article can be found online at http://dx.doi.org/10.1016/j.bone.2017.04.003.

Acknowledgements

This study was supported by HKU Seed Funding Programme for Basic Research (201511159033).

Authors' roles: CL, CZ and YY conceptualized the study. CL, SW and TC designed experiments and collected data. CL drafted the manuscript. TC, CZ, LJ and YY reviewed the data and edited the manuscript. All authors approved the final version of the manuscript.

References

[1] H. Xie, Z. Cui, L. Wang, Z.Y. Xia, Y. Hu, L.L. Xian, C.J. Li, L. Xie, J. Crane, M. Wan, G.H. Zhen, Q. Bian, B. Yu, W.Z. Chang, T. Qiu, M. Pickarski, L.T. Duong, J.J. Windle, X.H. Luo, E.Y. Liao, X. Cao, PDGF-BB secreted by preosteoclasts induces angiogenesis during coupling with osteogenesis, Nat. Med. 20 (2014) 1270–1278.
[2] T. Bellido, Osteocyte-driven bone remodeling, Calcif. Tissue Int. 94 (2014) 25–34.
[3] L.D. You, S. Temiyasathit, P.L. Lee, C.H. Kim, P. Tummala, W. Yao, W. Kingery, A.M. Malone, R.Y. Kwon, C.R. Jacobs, Osteocytes as mechanosensors in the inhibition of bone resorption due to mechanical loading, Bone 42 (2008) 172–179.
[4] P.S. Vezeridis, C.M. Semeins, Q. Chen, J. Klein-Nulend, Osteocytes subjected to pulsating fluid flow regulate osteoblast proliferation and differentiation, Biochem. Biophys. Res. Commun. 348 (2006) 1082–1088.
[5] F. Zhang, C.L. Wang, Y. Koyama, N. Mitsui, C. Shionome, R. Sanuki, N. Suzuki, K. Mayahara, N. Shimizu, M. Maeno, Compressive force stimulates the gene expression of IL-17s and their receptors in MC3T3-E1 cells, Connect. Tissue Res. 51 (2010) 359–369.
[6] I.E. Adamopoulos, E.P. Bowman, Immune regulation of bone loss by Th17 cells, Arthritis Res. Ther. 10 (2008) 255.
[7] I.E. Adamopoulos, C.C. Chao, R. Geissler, D. Laface, W. Blumenschein, Y. Iwakura, T. McClanahan, E.P. Bowman, Interleukin-17A upregulates receptor activator of NF-κB on osteoclast precursors, Arthritis Res. Ther. 12 (2010) R29.
[8] F. Shen, M.J. Ruddy, P. Plamondon, S.L. Gaffen, Cytokines link osteoblasts and inflammation: microarray analysis of interleukin-17-and TNF-α-induced genes in bone cells, J. Leukoc. Biol. 77 (2005) 388–399.
[9] F. Zhang, H. Tanaka, T. Kawato, S. Kitami, K. Nakai, M. Motohashi, N. Suzuki, C.L. Wang, K. Ochiai, K. Isokawa, M. Maeno, Interleukin-17A induces cathepsin K and MMP-9 expression in osteoclasts via celecoxib-blocked prostaglandin E_2 in osteoblasts, Biochimie 93 (2011) 296–305.
[10] E. Lubberts, M.I. Koenders, B. Oppers-Walgreen, L. van den Bersselaar, C.J.J. Coenen-de Roo, L.A.B. Joosten, W.B. van den Berg, Treatment with a neutralizing anti-murine interleukin-17 antibody after the onset of collagen-induced arthritis reduces joint inflammation, cartilage destruction, and bone erosion, Arthritis Rheum. 50 (2004) 650–659.
[11] C. Zhao, N. Irie, Y. Takada, K. Shimoda, T. Miyamoto, T. Nishiwaki, T. Suda, K. Matsuo, Bidirectional ephrinB2-EphB4 signaling controls bone homeostasis, Cell Metab. 4 (2006) 111–121.
[12] N. Irie, Y. Takada, Y. Watanabe, Y. Matsuzaki, C. Naruse, M. Asano, Y. Iwakura, T. Suda, K. Matsuo, Bidirectional signaling through EphrinA2-EphA2 enhances osteoclastogenesis and suppresses osteoblastogenesis, J. Biol. Chem. 284 (2009) 14637–14644.
[13] H. Huang, H.J. Kim, E.J. Chang, Z.H. Lee, S.J. Hwang, H.M. Kim, Y. Lee, H.H. Kim, IL-17 stimulates the proliferation and differentiation of human mesenchymal stem cells: implications for bone remodeling, Cell Death Differ. 16 (2009) 1332–1343.
[14] P. Miossec, J.K. Kolls, Targeting IL-17 and T(H)17 cells in chronic inflammation, Nat. Rev. Drug Dsicov. 11 (2012) 763–776.
[15] X.X.O. Yang, A.D. Panopoulos, R. Nurieva, S.H. Chang, D.M. Wang, S.S. Watowich, C. Dong, STAT3 regulates cytokine-mediated generation of inflammatory helper T cells, J. Biol. Chem. 282 (2007) 9358–9363.
[16] M.L. Cho, J.W. Kang, Y.M. Moon, H.J. Nam, J.Y. Jhun, S.B. Heo, H.T. Jin, S.Y. Min, J.H. Ju, K.S. Park, Y.G. Cho, C.H. Yoon, S.H. Park, Y.C. Sung, H.Y. Kim, STAT3 and NF-κB signal pathway is required for IL-23-mediated IL-17 production in spontaneous arthritis animal model IL-1 receptor antagonist-deficient mice, J. Immunol. 176 (2006) 5652–5661.

[17] L.F. Bonewald, Establishment and characterization of an osteocyte-like cell line, MLO-Y4, J. Bone Miner. Metab. 17 (1999) 61–65.
[18] J. Rosser, L.F. Bonewald, Studying osteocyte function using the cell lines MLO-Y4 and MLO-A5, Methods Mol. Biol. 816 (2012) 67–81.
[19] L.Y. Wang, C. Ciani, S.B. Doty, S.P. Fritton, Delineating bone's interstitial fluid pathway in vivo, Bone 34 (2004) 499–509.
[20] C.H. Kim, L. You, C.E. Yellowley, C.R. Jacobs, Oscillatory fluid flow-induced shear stress decreases osteoclastogenesis through RANKL and OPG signaling, Bone 39 (2006) 1043–1047.
[21] M.A. Kamel, J.L. Picconi, N. Lara-Castillo, M.L. Johnson, Activation of β-catenin signaling in MLO-Y4 osteocytic cells versus 2T3 osteoblastic cells by fluid flow shear stress and PGE_2: implications for the study of mechanosensation in bone, Bone 47 (2010) 872–881.
[22] J. Weischenfeldt, B. Porse, Bone marrow-derived macrophages (BMM): isolation and applications, CSH Protoc. 2008 (2008) (pdb.prot5080).
[23] D.K. Fogg, C. Sibon, C. Miled, S. Jung, P. Aucouturier, D.R. Littman, A. Cumamo, F. Geissmann, A clonogenic bone marrow progenitor specific for macrophages and dendritic cells, Science 311 (2006) 83–87.
[24] N. Huynh, L. VonMoss, D. Smith, I. Rahman, M.F. Felemban, J. Zuo, W.J. Rody, K.P. McHugh, L.S. Holliday, Characterization of regulatory extracellular vesicles from osteoclasts, J. Dent. Res. 95 (2016) 673–679.
[25] D.A. Ostrov, A.T. Magis, T.J. Wronski, E.K.L. Chan, E.J. Toro, R.E. Donatelli, K. Sajek, I.N. Haroun, M.I. Nagib, A. Piedrahita, A. Harris, L.S. Holliday, Identification of enoxacin as an inhibitor of osteoclast formation and bone resorption by structure-based virtual screening, J. Med. Chem. 52 (2009) 5144–5151.
[26] C. Chen, L. Kang, S. Chen, S. Hung, Y. Fu, H. Huang, (−)-Epigallocatechin-3-Gallate (EGCG) increases osteogenic differentiation of human bone marrow stromal cells, Bone 44 (2009) S296–S297.
[27] T. Hirata, Y. Osuga, K. Harnasaki, O. Yoshino, M. Ito, A. Hasegawa, Y. Takemura, Y. Hirota, E. Nose, C. Morimoto, M. Harada, K. Koga, T. Tajima, S. Saito, T. Yano, Y. Taketani, Interleukin (IL)-17A stimulates IL-8 secretion, cyclooxygensase-2 expression, and cell proliferation of endometriotic stromal cells, Endocrinology 149 (2008) 1260–1267.
[28] D. Inoue, M. Numasaki, M. Watanabe, H. Kubo, T. Sasaki, H. Yasuda, M. Yamaya, H. Sasaki, IL-17A promotes the growth of airway epithelial cells through ERK-dependent signaling pathway, Biochem. Biophys. Res. Commun. 347 (2006) 852–858.
[29] E. Lubberts, The IL-23-IL-17 axis in inflammatory arthritis, Nat. Rev. Rheumatol. 11 (2015) 415–429.
[30] W.J. Boyle, W.S. Simonet, D.L. Lacey, Osteoclast differentiation and activation, Nature 423 (2003) 337–342.
[31] J.M.W. Quinn, M.T. Gillespie, Modulation of osteoclast formation, Biochem. Biophys. Res. Commun. 328 (2005) 739–745.
[32] A. Hikita, I. Yana, H. Wakeyama, M. Nakamura, Y. Kadono, Y. Oshima, K. Nakamura, M. Seiki, S. Tanaka, Negative regulation of osteoclastogenesis by ectodomain shedding of receptor activator of NF-κB ligand, J. Biol. Chem. 281 (2006) 36846–36855.
[33] S. Zhao, Y. Kato, Y. Zhang, S. Harris, S.S. Ahuja, L.F. Bonewald, MLO-Y4 osteocyte-like cells support osteoclast formation and activation, J. Bone Miner. Res. 17 (2002) 2068–2079.
[34] T. Yago, Y. Nanke, N. Ichikawa, T. Kobashigawa, M. Mogi, N. Kamatani, S. Kotake, IL-17 induces osteoclastogenesis from human monocytes alone in the absence of osteoblasts, which is potently inhibited by anti-TNF-α antibody: a novel mechanism of osteoclastogenesis by IL-17, J. Cell. Biochem. 108 (2009) 947–955.
[35] K. Gordon, J.J. Kochkodan, H. Blatt, S.Y. Lin, N. Kaplan, A. Johnston, W.R. Swindell, P. Hoover, B.J. Schlosser, J.T. Elder, J.E. Gudjonsson, S. Getsios, Alteration of the EphA2/Ephrin-A signaling axis in psoriatic epidermis, J. Invest. Dermatol. 133 (2013) 712–722.
[36] K. Diercke, S. Sen, A. Kohl, C.J. Lux, R. Erber, Compression-dependent up-regulation of Ephrin-A2 in PDL fibroblasts attenuates osteogenesis, J. Dent. Res. 90 (2011) 1108–1115.
[37] K. Diercke, A. Kohl, C.J. Lux, R. Erber, Strain-dependent up-regulation of EphrinB2 protein in periodontal ligament fibroblasts contributes to osteogenesis during tooth movement, J. Biol. Chem. 286 (2011) 37651–37664.
[38] A. Jager, D.L. Zhang, A. Kawarizadeh, R. Tolba, B. Braumann, S. Lossdorfer, W. Gotz, Soluble cytokine receptor treatment in experimental orthodontic tooth movement in the rat, Eur. J. Orthod. 27 (2005) 1–11.
[39] J. Surapisitchat, R.J. Hoefen, X.C. Pi, M. Yoshizumi, C. Yan, B.C. Berk, Fluid shear stress inhibits TNF-α activation of JNK but not ERK1/2 or p38 in human umbilical vein endothelial cells: inhibitory crosstalk among MAPK family members, Proc. Natl. Acad. Sci. U. S. A. 98 (2001) 6476–6481.
[40] H.K. Zhou, A.B. Newnum, J.R. Martin, P. Li, M.T. Nelson, A. Moh, X.Y. Fu, H. Yokota, J.L. Li, TATOsteoblast/osteocyte-specific inactivation of STAT3 decreases load-driven bone formation and accumulates reactive oxygen species, Bone 49 (2011) 404–411.
[41] C.A. O'Brien, I. Gubrij, S.C. Lin, R.L. Saylors, S.C. Manolagas, STAT3 activation in stromal osteoblastic cells is required for induction of the receptor activator of NF-κB ligand and stimulation of osteoclastogenesis by gp130-utilizing cytokines or interleukin-1 but not 1,25-dihydroxyvitamin D_3 or parathyroid hormone, J. Biol. Chem. 274 (1999) 19301–19308.
[42] M. Croes, F.C. Oner, D. van Neerven, E. Sabir, M.C. Kruyt, T.J. Blokhuis, W.J.A. Dhert, J. Alblas, Proinflammatory T cells and IL-17 stimulate osteoblast differentiation, Bone (2016) 262–270.